

# Photoacoustic Microscopy for biomedical Application

**Abstract: The** main aim of the project is to build a microscopy device to for tissue imaging by photoacoustic effect technique which combines the ultrasound imaging and optical imaging to achieve better imaging depth, resolution, contrast, in the point of view of medical interest. In my report I will be discussing first the photoacoustic effect, then varies types of imaging technics adapted with this effect, then I will be mainly focusing on photoacoustic microscopy types and then instrumentation, experiments and finally am writing my contribution in this project.

## Introduction

The photoacoustic imaging is Well situated to microscopic and macroscopic domains in the life sciences. In this, we get the advantage of Conversion of optical energy into acoustic energy in terms of depth of imaging and the resolution of the image. With this technique, one can characterize the functional, metabolic, histologic properties and from molecular to cellular imaging can be done. It is complementary to and compatible (mainly with optical and ultrasound imaging). It is non-hazardous (non-ionizing, non-destructive, non-invasive) and safety to health.

## Photoacoustic effect

The generation of sound waves due to absorption of light, a short duration, in a sample material was first discovered by Alexander Graham Bell in 1880. The photoacoustic effect or optoacoustic effect is the formation of sound waves following light absorption in a material sample. In order to obtain this effect, the light intensity must vary, either periodically (modulated light) or as a single flash

there are actually several different mechanisms that produce the photoacoustic effect. The primary universal mechanism is photothermal, based on the heating effect of the light and the consequent expansion of the light-absorbing material. In detail, the photothermal mechanism consists of the following stages:

1. conversion of the absorbed pulsed or modulated radiation into heat energy.
2. temporal changes of the temperatures at the loci where radiation is absorbed – rising as radiation is absorbed and falling when radiation stops and the system cools.
3. expansion and contraction following these temperature changes, which are "translated" to pressure changes. The pressure changes, which occur in the region where the light was absorbed, propagate within the sample body and can be sensed by a sensor coupled directly to it. Commonly, for the case of a condensed phase sample (liquid, solid), pressure changes are rather measured in the surrounding gaseous phase (commonly air), formed there by the diffusion of the thermal pulsations.

## The principle of photoacoustic imaging (PAI)

The generation of sound waves due to absorption of light, a short duration, in a sample material was first discovered by Alexander Graham Bell in 1880 and by using this effect first time in 1990 The laser-induced counterpart of 1D depth-resolved imaging has reported.

“A short a short laser pulse fired at the biological tissue. As photons propagate into the tissue, some are absorbed by biomolecules. The absorbed optical energy is usually partially or completely converted into heat through nonradiative relaxation of excited molecules. The heat-induced pressure wave propagates in tissue as an ultrasound wave. The ultrasound wave is detected outside the tissue by an ultrasonic transducer or transducer array to form an image that maps the original optical energy deposition inside the tissue.”

### 1.1. Signal generation in PAI

To generate acoustic waves, the thermal expansion needs to be time variant. This requirement can be achieved by using either a pulsed laser or a continuous-wave (CW) laser with intensity modulation at a constant or variable frequency. Pulsed excitations are the most widely used because they provide a higher signal to noise ratio than CW excitations. Following a short laser pulse excitation, the local fractional volume expansion  $\frac{dV}{V}$  can be expressed as

$$\frac{dV}{V} = -\kappa p(\vec{r}) + \beta T(\vec{r}) \quad (1)$$

where  $\kappa$  is the isothermal compressibility,  $\beta$  is the thermal coefficient of volume expansion, and  $p(\vec{r})$  and  $T(\vec{r})$  are changes in pressure and temperature, respectively.

For effective PAT signal generation, the laser pulse duration is normally within several nanoseconds, which is less than both the thermal and stress confinement times. The thermal confinement indicates that thermal diffusion during laser illumination can be neglected, i.e., [53]

$$\tau < \tau_{th} = \frac{d_c^2}{4D_T} \quad (2)$$

Here,  $\tau_{th}$  is the thermal confinement threshold,  $d_c$  is the desired spatial resolution, and  $D_T$  is the thermal diffusivity.

The stress confinement means the volume expansion of the absorber during the illumination period can be neglected. This condition can be written as

$$\tau < \tau_{st} = \frac{d_c}{v_s} \quad (3)$$

where  $v_s$  is the speed of sound.

For a 100  $\mu\text{m}$  spatial resolution, the thermal confinement time is 18 ms and the stress confinement time is 67 ns. A typical pulsed laser has a pulse duration of only 10 ns. In this case, the fractional volume expansion in Eq. (1) is negligible and the initial photoacoustic pressure  $p_0(\vec{r})$  can be written as

$$p_0(\vec{r}) = \frac{\beta T(\vec{r})}{\kappa} \quad (4)$$

For soft tissue,  $\kappa$  is approximately  $5 \times 10^{-10} \text{ Pa}^{-1}$  and  $\beta$  is around  $4 \times 10^{-4} \text{ K}^{-1}$ . Thus each mK temperature rise generates an 800 Pa pressure rise, which is detectable ultrasonically. The temperature rise can be further expressed as a function of optical absorption,

$$T = \frac{A_e}{\rho C_V} \quad (5)$$

Here  $\rho$  is the mass density,  $C_V$  is the specific heat capacity at constant volume, and  $A_e$  is the absorbed energy density, which is a product of the absorption coefficient  $\mu_a$  and the local optical fluence  $F(r^{\rightarrow})$ .

Based on Eqs. (4) and (5), the initial photoacoustic pressure can be written as

$$p_0(r^{\rightarrow}) = \frac{\beta A_e}{\rho C_V \kappa} = \Gamma \mu_a F(r^{\rightarrow}) \quad (6)$$

Here  $\Gamma(r^{\rightarrow}) = \beta / \rho C_V \kappa$  is the Grueneisen parameter, which increases as the temperature rises. Thus, PAT can also be used to monitor temperature. Eq. (6) indicates that, to extract the object's absorption coefficient from pressure measurements, the local fluence  $F(r^{\rightarrow})$  needs to be quantified.

Once the initial pressure  $p_0(r^{\rightarrow})$  is generated, it splits into two waves with equal magnitude, traveling in opposite directions. The shape of the wave front depends on the geometry of the object. For a spherical object, two spherical waves will be generated: one travels outward, and the other travels inward as compression followed by rarefaction. Thus, the photoacoustic signal has a bipolar shape and the distance between the two peaks is proportional to the size of the object. In other words, a smaller object generates a photoacoustic signal with higher frequency components.

The generated photoacoustic pressure propagates through the sample and is detected by an ultrasonic transducer or transducer array. The goal of photoacoustic image formation is to recover the distribution of  $p_0(r^{\rightarrow})$  from the time-resolved ultrasonic signals.

## 2.2. Image formation in PAI

Based on the image formation methods, PAT has two major implementations [2]. The first, direct image formation, is based on mechanical scanning of a focused single-element ultrasonic transducer and is commonly used in photoacoustic microscopy (PAM). The second, reconstruction image formation, is based on mechanical/electronic scanning of a multi-element transducer array and is used in photoacoustic computed tomography (PACT). In PAM, the received photoacoustic signal originates primarily from the volume laterally confined by the acoustic focus and can be simply converted into a one-dimensional image along the acoustic axis. In PACT, each transducer element has a large acceptance angle within the field of view, and a PA image can only be reconstructed only by merging data from all transducer elements. In the following, we will discuss PACT image reconstruction in detail.

For an ideal point transducer placed at  $r_d^{\rightarrow}$ , the detected photoacoustic signal can be written as

$$p_d(\vec{r}_d, t) = \frac{\partial}{\partial t} \left[ \frac{t}{4\pi} \iint_{|\vec{r}_d - \vec{r}| = v_s t} p_0(\vec{r}) d\Omega \right] \quad (7)$$

Here,  $d\Omega$  is the solid-angle element of  $\vec{r}$  with respect to the point at  $\vec{r}_d$ , and  $v_s$  is the speed of sound. Eq. (7) indicates that the detected pressure at time  $t$  comes from sources over a spherical shell centered at the detector position  $\vec{r}_d$  with a radius  $v_s t$ . The initial pressure distribution  $p_0(\vec{r})$  can be obtained by inverting Eq. (7). For spherical, planar, and cylindrical detection geometries, exact inversion solutions have been provided by Xu et al. The so-called universal back-projection (UBP) algorithm can be expressed in the temporal domain as:

$$p_0(\vec{r}) = \frac{1}{\Omega_0} \int_S d\Omega \left[ 2p_d(\vec{r}_d, t) - 2t \frac{\partial p_d(\vec{r}_d, t)}{\partial t} \right] \Big|_{t=|\vec{r}_d - \vec{r}|/C} \quad (8)$$

Here,  $\Omega_0$  is the solid angle of the whole detection surface  $S$  with respect to a given source point at  $\vec{r}$ . Eq. (8) indicates that  $p_0(\vec{r})$  can be obtained by back-projecting the filtered data,  $[2p_d(\vec{r}_d, t) - 2t \partial p_d(\vec{r}_d, t) / \partial t]$ , onto a collection of concentric spherical surfaces that are centered at each transducer location  $\vec{r}_d$ , with  $d\Omega / \Omega_0$  as the weighting factor applied to each back-projection.

## Photoacoustic Microscopy

Photoacoustic microscopy (PAM) is the major implementation of PAT, which images targets in the (quasi)ballistic and quasi-diffusive regimes at a high spatial resolution at depths. the most significant difference between PAM and PACT is that PAM uses a focused single-element ultrasonic transducer for direct image formation, while PACT typically uses a multi-element transducer array or its equivalent for digital image reconstruction. The lateral resolution of PAM is determined by the product of the point spread functions of the light illumination and acoustic detection. The axial resolution of PAM is determined by the detection bandwidth of the ultrasonic transducer, which is chosen to match the acoustic path length due to frequency-dependent acoustic attenuation in tissue. PAM can divide majorly into two. First **optical resolution PAM** (OR PAM) where the optical focus is much tighter than the acoustic focus. The optical beam can be easily focused to a much tighter spot than the acoustic detection. Imaging depth can be reached up to 1mm. another one is **Acoustic-resolution PAM** (AR PAM) where the Acoustic focus is tighter than the diffused optical beam. Can achieve better focusing, taking advantage of the weaker acoustic scattering. Imaging depth is up to 1cm to 4cm. This two can be operated in a different mode as shown in figure2. The scalability of PAM originates from its optical and acoustic focusing. Within the optical diffusion limit, OR-PAM has a great advantage over AR-PAM in spatial resolution because the optical beam can be easily focused to a much tighter spot than the acoustic detection, owing to shorter optical wavelengths. Beyond the optical diffusion limit, however, AR-PAM can achieve better focusing, taking advantage of the weaker acoustic scattering.

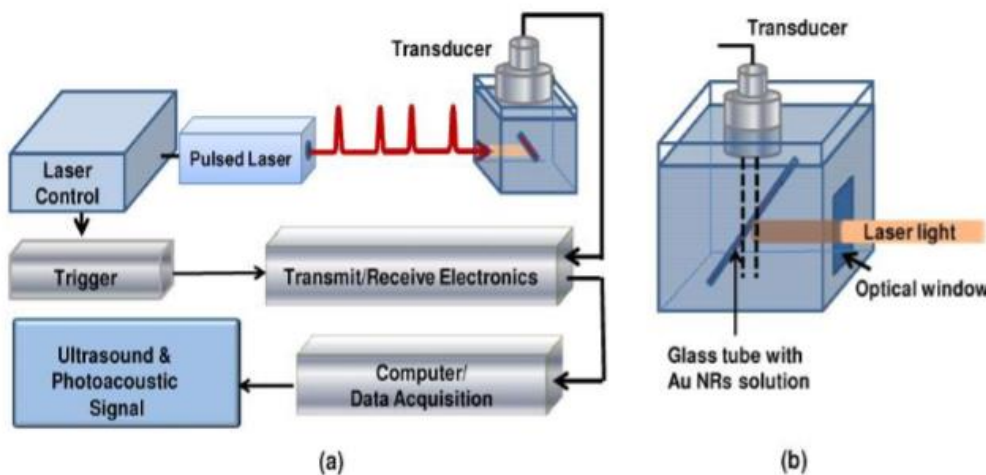


Fig: (a) A block diagram of the ultrasound and photoacoustic imaging system; (b) ultrasonic transducer as a detector

### Major PAI implementations

- a short-pulsed laser for efficient wideband PA signal generation
- a wideband ultrasonic transducer or transducer array for signal detection
- a data acquisition system for signal amplification and digitization
- a computer for system synchronization, data collection, and image formation

### 3.1. Methodology

a short laser of the pulse of laser light with width 6 nsec with relatively high intensity is allowed to irradiate to a specific region of interest to a tissue. The process is governed by propagation of electromagnetic waves in a medium and hence characterized by optical properties of the propagating medium namely, optical absorption scattering and refractive index. Due to that deposition of optical energy white light is propagated through a medium and the absorbed energy is converted into heat by vibrational and oscillations motion, it further helps the temperature to rise to a certain amount and when temperature raises thermoelastic expansion comes into the effect. Therefore it induces a transient raise in pressure. A parameter such as absorption coefficient, optical fluence, density and specific heat capacity at constant volume all together gives an initial temperature rise in the tissue wherein irradiated by a certain amount of light. Further parameters such as grunesen parameter, specific heat at constant pressure, thermal coefficient of expansion, specific optical absorption give an account to rise in pressure therefore initial pressure rise denoted by  $P_0$  depends upon the thermoelastic expansion and photoacoustic effect. The elastic property comes into an effect in the phenomenon thereby target region and the background is related with a strain in which target acts as a change in length and background, the strain induced will be lower and vice versa. In photoacoustic imaging, the acoustic signals with frequencies of the order 30 MHz are employed and selectively picked up using an ultrasonic transducer as a detector and the tissue material properties are derived from the ultrasound signals detected at the boundary.

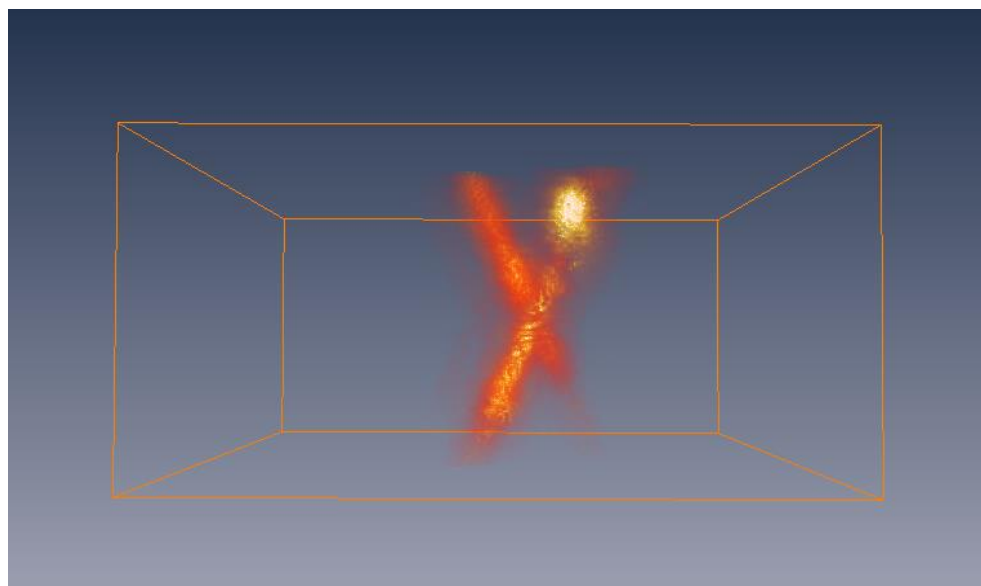
In our experiment copper wire mesh as sample, a light of laser pulse width 6 nsec, wavelength 720nm and energy density of 22 mJ/cm<sup>2</sup> is passed on it. A tightly focusing ultrasound transducer was kept in the sample boundary to pick up the laser-induced PA signals,

selectively, from the narrow focal region of the transducer. To get proper coupling of ultrasound transmission and its efficient detection, the transducer is allowed to immerse in water ( but not fully deep inside the water and it is not in contact with the sample, a lab jack is used to raise up) the sample therefore was kept in a fixed position below the water container. Again for proper coupling of ultrasound transmission from the tissue surface to the water medium, the water container was cut out so as to fit the sample. The cutout portion was covered with an optically transparent polyethylene membrane to avoid leakage of water while providing proper coupling of ultrasound transmission. Additionally, an acoustic coupling gel was applied over the surface of the sample for further improvement in ultrasound transmission. In this way, one can say that the sample is virtually immersed in the acoustic-coupling medium. An A-scan data was obtained by collecting a sequence of time-resolved PA-signals employing a data acquisition (DAQ) hardware by picking up an array of PA-signals acting as an individual point source, along a line in the direction of the transducer axis rather than mapping of acoustic impedance from reflection at tissue interfaces separating tissue layers of different acoustic properties. Signals focusing transducer with axial resolution being determined by DAQ sampling frequency while the lateral resolution is determined by the focal spot size of the transducer. In PAM<sub>3</sub> the contrast of the detected PA-signals results from a variation in the distribution of optical and mechanical properties at a microscopic resolution not from a mismatched acoustic impedances of tissue layers being separated by an interface.

Data acquisition: samples are kept at fix position during experimentation and 3D Scanning is done wherein the ultrasound detecting transducer and optical fibers, was translated in the horizontal XY plane. A focused ultrasonic transducer of central frequency(30MHz) was used to pick up the light-stimulated PA signals from the narrow focal region and an A-scan data was provided by a time-resolved PA signal being detected at scanning position, further B-scan image was obtained by raster scanning of the sample along a horizontal axis (x-axis) and extended along another horizontal axis (y-axis) perpendicular to x-axis, thus obtained a 3D image. So by raster scanning, a 3D/2D images were obtained. This process was carried by the implementation of LabVIEW software. Image reconstruction algorithm has been developed for obtaining 3D/2D images from the collected data and so constructed the images.

## Results

Fig: 3D  
Reconstructed  
image of  
copper wire  
obtained



## Conclusion and Discussion

The requirement for obtaining images from photoacoustic signals through certain methods has been developed. The LabVIEW software has learned so it can be utilized in other areas too. The process and principle of PAM has been understood with respect to all of its parameters. In future this understanding will be used for LED based PAM, very short pulse duration of tens of nanoseconds was made possible by the fast response of the LED and the high-speed driving. Which will be more convenient to bring it in clinical as real time imaging system. Apart from that certain experiments can be done using different samples and check the resolution power under certain depths in photoacoustic domain.

## References

1. M. Suheshkumar Singh and H. Jiang, "Estimating both direction and magnitude of flow velocity using photoacoustic microscopy," Appl. Phys. Lett. (in press).
2. M. Suheshkumar Singh and H. Jiang, "Elastic property attributes to photoacoustic signals: an experimental phantom study" Optics. Lett. vol.39, No. 13 (2014)
3. M. Suheshkumar Singh and H. Jiang "Ultrasound (US) transducer of higher operating frequency detects photoacoustic (PA) signals due to the contrast in elastic property" 54
4. Xose Luis Dea n-Ben1, Erwin Bay & Daniel Razansky " Functional optoacoustic imaging of moving objects using the microsecond-delay acquisition of multispectral three-dimensional tomographic data"
5. Junjie Yao and Lihong V. Wang "Photoacoustic microscopy" Laser Photonics Rev. 7, No. 5, 758–778 (2013)
6. Lihong V Wang & Junjie Yao "A practical guide to photoacoustic tomography in the life sciences " nature methods Vol.13 No.8 Aug (2016)
7. Paul beard "Biomedical Photoacoustic imaging" Interface focus (2011) 1, 602–631.
8. Junjie Yao, Lihong V Wang "Sensitivity of photoacoustic microscopy" Photoacoustics 2 (2014) 87-101
9. Sung-Liang Chen, L Jay Guo, Xueding Wang "All-Optical photoacoustic Microscopy " Photoacoustic 3 (2015) 143-150
10. Wang LV. Multiscale photoacoustic microscopy and computed tomography. Nat Photon. 2009;3:503–509
11. Wang LV, Hu S. Photoacoustic Tomography: In Vivo Imaging from Organelles to Organs. Science. 2012 Mar 23;335:1458–1462. 2012
12. Yunhao Zhu1, Guan Xu, Jie Yuan, Janggun Jo, Girish Gandikota, Hakan Demirci, Toshitaka Agano, Naoto Sato, Yusuke Shigeta & Xueding Wang "Light Emitting Diodes based Photoacoustic Imaging and Potential Clinical Applications". Scientific reports 2018
13. Thomas J. Allen\* and Paul C. Beard "High power visible light emitting diodes as pulsed excitation sources for biomedical photoacoustics" biomedical optics express 2016
14. Yao JJ, Wang LHV. Photoacoustic microscopy. Laser & Photonics Reviews. 2013 Sep;7:758–778
15. Wang X, Pang Y, Ku G, Xie X, Stoica G, Wang LV "Noninvasive laser-induced photoacoustic tomography for structural and functional in vivo imaging of the brain." Nat Biotechnol. 2003 Jul; 21(7):803-6.

**Project Supervisor**  
**Dr. Suhesh Kumar Singh**  
**School of physics IISER-TVM**

**Submitted by**  
**B Kalyan Singh**  
**IMS14039**

